Different types of Na^+ and A-type K^+ currents in dorsal root ganglion neurones innervating the rat urinary bladder

Naoki Yoshimura, Geoffrey White*, Forrest F. Weight* and William C. de Groat

*Department of Pharmacology, School of Medicine, University of Pittsburgh, Pittsburgh, PA 15261, USA and *Section of Electrophysiology, Laboratory of Physiologic and Pharmacologic Studies, National Institute on Alcohol Abuse and Alcoholism, Rockville, MD 20892, USA*

1. Whole-cell patch-clamp recording in combination with axonal tracing techniques was used to examine the electrical properties of afferent neurones innervating the urinary bladder of the adult rat. Individual bladder afferent cells were labelled by Fast Blue (FB), injected into the bladder wall.

2. Passive and active electrical parameters at room temperature (20–22 °C) in FB-labelled bladder afferent neurones were comparable with those in unlabelled neurones. Unselected dorsal root ganglion (DRG) neurones as well as bladder afferent neurones exhibited two different types of action potential: high-threshold humped spikes in small-sized neurones and low-threshold narrow spikes in large-sized neurones.

3. The majority (70%) of bladder neurones which were small in size expressed high-threshold tetrodotoxin (TTX)-resistant Na^+ channels and slow-inactivating A-type K^+ channels (K_A), which were available at the resting membrane potential, whereas large-sized DRG neurones had low-threshold TTX-sensitive Na^+ channels and fast-inactivating K_A channels, which were almost completely inactivated at the resting membrane potential.

4. Half-maximal conductances of activation of TTX-resistant and TTX-sensitive Na^+ currents were obtained at −10·3 and −25·3 mV, respectively. The TTX-resistant and TTX-sensitive Na^+ currents were half-inactivated at −25·3 and −56 mV, respectively.

5. In the TTX-resistant neurones, the transient outward K^+ current (A-type current, I_A) with half-maximal conductance at −40·8 mV was half-inactivated at −77·5 mV, and exhibited slower decaying kinetics (mean decay constant (τ), 240 ms) than the I_A current recorded from the large-sized TTX-sensitive neurones (mean τ, 20 ms).

6. These results suggest that the majority of bladder afferent neurones have high electrical thresholds for spike activation due to the TTX-resistant Na^+ current and the slow-inactivating I_A current, which reflect the large population of unmyelinated high-threshold C fibre afferents that innervate the urinary bladder.

The sensory innervation of the urinary bladder consists of thin myelinated (Aδ) and unmyelinated (C) axons which travel in pelvic (parasympathetic) and hypogastric (sympathetic) nerves. The Aδ afferent axons in the pelvic nerve respond to low-threshold mechanical stimuli such as bladder distension (Mallory, Steers & de Groat, 1989; de Groat *et al.* 1990*a*; Jänig & Koltzenburg, 1990) and play a major role in the initiation of the micturition reflex (de Groat, Booth & Yoshimura, 1993). On the other hand, C fibre bladder afferents in cats do not respond to mechanical stimuli and thus have been termed 'silent C fibres' (de Groat *et al.* 1990*a*; Jänig & Koltzenburg, 1990). However, these C fibre afferents can be activated by chemical irritation (Habler, Jänig & Koltzenburg, 1990) or cold stimulation of the bladder (Fall, Lindström & Mazières, 1990) and can in turn facilitate the micturition reflex.

The present experiments were undertaken to examine the electrical properties of bladder afferent neurones in the adult rat using patch-clamp recording. Previous axonal tracing studies in the rat have demonstrated that the pelvic afferent innervation of the bladder arises from neurones in the L6 and S1 dorsal root ganglia (DRG) (Nadelhaft & Booth, 1984; de Groat *et al.* 1993). These neurones were labelled by retrograde axonal transport of a fluorescent dye injected into the urinary bladder and then individual dye-labelled neurones were identified by fluorescence microscopy after

chemical dissociation of the DRG (Christian, Togo, Naper, Koschorke, Taylor & Weinreich, 1993; Yoshimura, White, Weight & de Groat, 1994). Although many patch-clamp studies have been performed on isolated sensory neurones (Ikeda, Schofield & Weight, 1985; White, 1990; Ogata & Tatebayashi, 1992, 1993; Elliott & Elliott, 1993), relatively few have been conducted on target-specific neurones. Thus, the axonal labelling methods used in the present experiments allowed an investigation of an identified population of neurones to determine whether these neurones exhibit specific electrophysiological and pharmacological characteristics that correlate with the functional properties of bladder afferent pathways *in vivo*.

Preliminary reports of some of these observations have appeared in abstract form (de Groat, White & Weight, 1990*b*; Yoshimura & de Groat, 1992).

METHODS

Dorsal root ganglion cell preparation

The L6 and S1 DRG were removed from ketamine-anaesthetized (100–125 mg kg^{-1}, I.M.) male adult Sprague–Dawley rats (150–250 g) and then placed in 5 ml Dulbecco's modified Eagle's medium (DMEM; Sigma) containing 0·3 mg ml^{-1} trypsin (Sigma Type III), 1 mg ml^{-1} collagenase (Sigma Type IA) and 0·1 mg ml^{-1} deoxyribonuclease (DNase; Sigma Type III). Animals were killed by an overdose of anaesthetic. The DRG were agitated at 1–2 Hz in a shaking water-bath for 25–30 min at 35 °C. Following dissociation, soybean trypsin inhibitor (Sigma Type II) was added. Isolated neurones were maintained at room temperature (20–22 °C) in DMEM and allowed to attach to the bottom of culture dishes prior to patch-clamp recording. Cells were used for recording within 1–12 h after dissociation. Neuronal diameter was measured under a phase-contrast microscope using an eye-piece micrometer. Cell diameter was calculated from the average value of the long and short dimensions of the cells.

Dye labelling

The subpopulation of DRG neurones which innervate the urinary bladder was identified by labelling with retrograde axonal transport of a fluorescent dye (Fast Blue (FB), 4% (w/w); Polyloy, Grob-Umstadt, Germany) injected into the bladder wall 10–14 days prior to the dissociation. The procedure of dye injection has been described previously (Keast, Booth & de Groat, 1989). Briefly, under halothane anaesthesia, the urinary bladder was exposed by a mid-line incision using sterile technique and then three to six injections (total volume, 20–30 μl) were made into the dorsal surface of the bladder with a 28G needle. At each injection site the needle was kept in place for 20–30 s. The site was then rinsed with normal saline. No apparent leakage of dye was observed. The abdominal incision was closed and the animal was allowed to recover from anaesthesia. The experimental protocols were approved by the University of Pittsburgh Institutional Animal Care and Use Committee. After the DRG were dissociated into single neurones, FB-labelled bladder afferent neurones were identified with a Nikon inverted microscope with phase-contrast and fluorescence attachments (UV-1A filter; excitation wavelength, 365 nm). During identification, the neurones were exposed to UV light for only short periods (10–15 s) since exposure for longer than 1 min changed the electrical properties of FB-labelled cells (Yoshimura *et al.* 1994). In some experiments, animals ($n = 4$) were pretreated 4 days prior to dye injection with capsaicin, a neurotoxin which is known to disrupt the function of C fibre afferents (Holtzer, 1991) and which markedly diminishes the number of DRG neurones labelled by axonal transport of tracers from the urinary bladder (Steers, Ciambotti, Etzel, Erdman & de Groat, 1991). It was therefore assumed that FB-labelled neurones obtained after capsaicin treatment would consist mainly of Aδ fibre bladder afferent cells. Capsaicin, which was dissolved in physiological saline containing 10% ethanol and 10% Tween 80 (v/v), was injected subcutaneously (total dose, 125 mg kg^{-1}) in divided doses on two consecutive days in animals under halothane anaesthesia (Cheng, Ma & de Groat, 1995). Desensitization to capsaicin was examined by eye-wipe test (Gamse, Leeman, Holtzer & Lembeck, 1982) prior to dye injections.

Electrical recording

Whole-cell patch-clamp recordings (Hamill, Marty, Neher, Sakmann & Sigworth, 1981) on isolated neurones were performed with an Axopatch-1D patch-clamp amplifier (Axon Instruments) connected to a digital computer through a Labmaster interface. Experiments were performed on neurones from uninjected rats and on dye-filled neurones from injected rats. Data were acquired and analysed with 'pCLAMP' software (Axon Instruments). For voltage-clamped recording, the filter was set to −3 dB at 2000 Hz. Leak current was subtracted by $P/4$ methods. Patch electrodes were fabricated from borosilicate capillary tubing, and had resistances of 1–4 MΩ when filled with internal solution. During recordings, neurones were superfused, at room temperature (20–22 °C) in a chamber with a volume of 2 ml, with balanced salt solution of varying composition at a flow rate of 1·5 ml min^{-1}. The normal external solution contained (mM): NaCl, 150; KCl, 5; $CaCl_2$, 2·5; $MgCl_2$, 1; Hepes, 10; and D-glucose, 10; adjusted to pH 7·4 with NaOH (340 mosmol l^{-1}). The normal internal solution contained (mM): KCl, 140; $CaCl_2$, 1; $MgCl_2$, 2; EGTA, 11; Hepes, 10; and Mg-ATP, 2; adjusted to pH 7·4 with KOH (310 mosmol l^{-1}). For isolation of Na^+ currents, the external solution contained (mM): NaCl, 100; TEA-Cl, 50; Hepes, 10; $MgCl_2$, 10; and D-glucose, 10; adjusted to pH 7·4 with NaOH (340 mosmol l^{-1}), and the internal solution contained (mM): CsCl, 115; NaCl, 25; Hepes, 10; $MgCl_2$, 3; and EGTA, 11; adjusted to pH 7·4 with CsOH (310 mosmol l^{-1}). Tetrodotoxin (TTX) and 4-aminopyridine (4-AP) were applied to the cell either by injection into the external solution or directly from a superfusion glass pipette (tip size, 15–25 μm) positioned close to the cell.

Results are given as means ± S.E.M.

RESULTS

Passive membrane properties and action potentials

Acutely dissociated neurones were spherical in shape and usually devoid of processes although some cells had short processes 3–5 μm in length. The cells varied in size from 15 to 50 μm in diameter, with most of the cells in the range 18–34 μm. Cells containing FB, which were labelled by injection of the dye into the urinary bladder, were readily detected with a epifluorescence illumination (Fig. 1). Current-clamp recordings were performed in normal solutions to examine the electrical and pharmacological properties of both unidentified DRG neurones and FB-labelled bladder afferent neurones. The mean resting membrane potentials were −58·9 ± 1·9 and −55·3 ± 1·8 mV in unidentified ($n = 44$) and dye-labelled ($n = 49$) neurones, respectively. Mean input resistances measured by injection of hyperpolarizing current through the pipette were 537·8 ± 46·2

and 581·0 ± 45·3 MΩ in unidentified and bladder afferent neurones, respectively. When depolarizing current pulses were injected into unidentified and bladder afferent cells through the pipette, action potentials were elicited with respective mean overshoots of 30·8 ± 5·2 and 36·8 ± 3·4 mV. Thus, the passive and active membrane parameters of FB-labelled cells did not differ from those of unidentified DRG neurones.

Unidentified and bladder afferent neurones were divided into two populations according to the characteristics of their action potentials. The most common population of unidentified and FB-labelled neurones had long-duration action potentials (9·1 ± 0·7 ms ($n = 28$) and 9·4 ± 0·5 ms ($n = 38$), respectively, measured at 50% of spike height) with an inflection on the repolarizing phase and mean thresholds of −20·4 ± 1·0 and −21·2 ± 0·9 mV for activation, respectively (Figs 2*A* and 3*A*). This type of cell was small in size with respective mean diameters of 22·6 ± 1·6 μm (range, 15–32 μm) and 24·2 ± 1·8 μm (range, 18–30 μm) for unidentified and FB-labelled cells. When Ca^{2+} was removed from the bathing solution, the inflection on the repolarizing phase of the action potentials disappeared, but the spike amplitude was not altered. The action potential remaining after removal of extracellular Ca^{2+} was unaltered by the application of TTX in concentrations up to 6 μM (Figs 2*B* and 3*B*) but was eliminated by removal of Na^+ ions from the external solution.

The second population of unidentified and FB-labelled neurones exhibited lower thresholds for spike activation (−35·1 ± 1·2 mV ($n = 16$) and −34·4 ± 3·5 mV ($n = 11$), respectively) and shorter duration action potentials (5·3 ± 0·9 and 5·6 ± 0·8 ms) than the first population of cells (Figs 2*C* and 3*C*). This type of unidentified and FB-labelled neurones rarely had an inflection on the repolarization phase of spikes and were larger in size, with respective mean diameters of 35·6 ± 1·6 μm (range, 30–47 μm) and 32·4 ± 1·2 μm (range, 29–35 μm), than those in the first population. The action potential in these neurones was reversibly blocked by application of 1 μM TTX (Figs 2*D* and 3*D*). There was no difference in mean resting membrane potential and input resistance between the two populations of neurones.

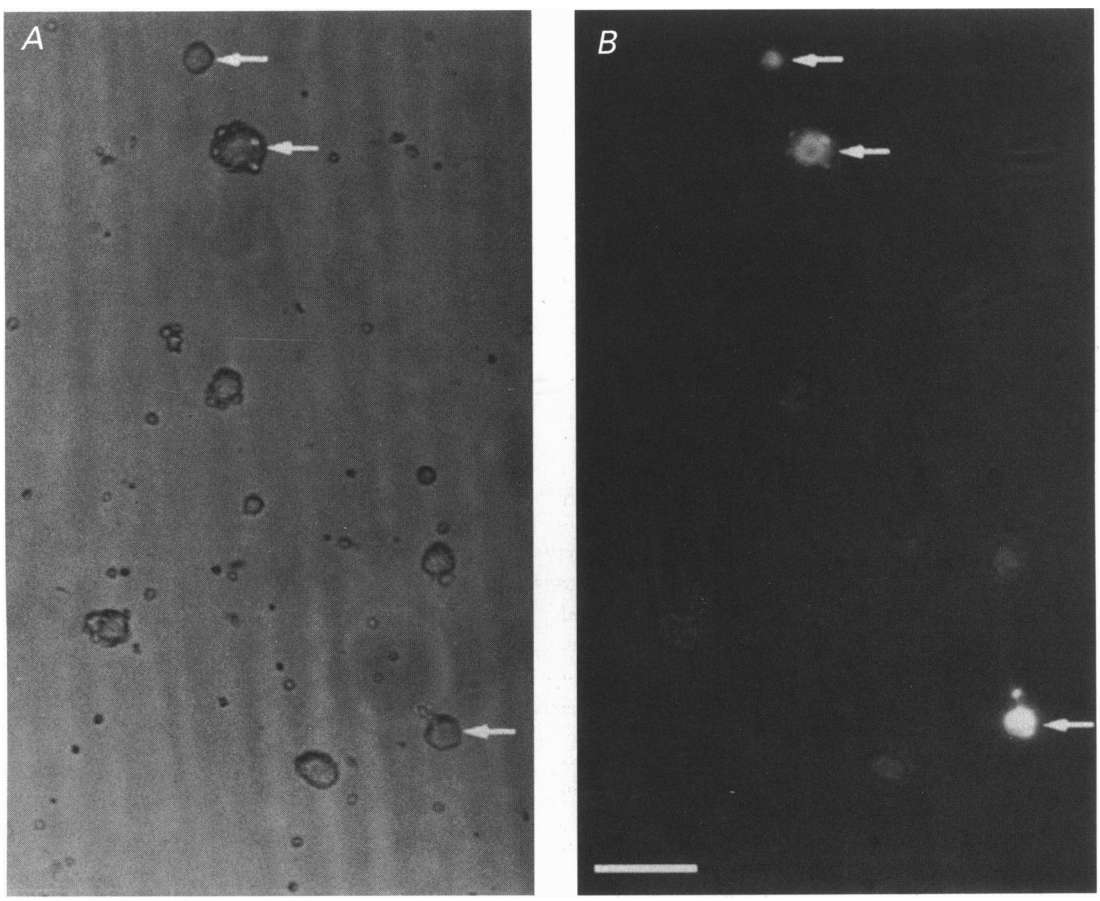

Figure 1. Photomicrographs of dissociated unlabelled and FB-labelled DRG cells

A, phase-contrast photomicrograph of DRG neurones. FB-labelled cells are indicated by arrows. *B*, fluorescence photomicrograph of the same field as in *A* showing 3 fluorescent DRG neurones (arrows). Scale bar, 100 μm.

In the animals pretreated with capsaicin, FB-labelled bladder afferent neurones ($n = 18$) were less numerous and were on average larger in diameter (32·3 ± 2·1 μm; range, 30–35 μm) than those from normal rats. Seventeen out of eighteen neurones exhibited TTX-sensitive short-duration (5·3 ± 0·4 ms) action potentials with low thresholds of activation (−31·1 ± 2·2 mV). The remaining neurone had a TTX-resistant humped, high-threshold action potential.

Effect of 4-AP on action potential threshold

The two populations of neurones could also be distinguished on the basis of the effect of 4-AP on action potential threshold. In small-sized neurones ($n = 4$) exhibiting TTX-resistant, high-threshold action potentials, administration of 4-AP (1 mM) shifted the threshold in the hyperpolarizing direction by an average of 6 mV (−21 to −27 mV; Fig. 4*A*) when tested on spikes initiated by depolarizing current pulses from holding potentials of −55 to −60 mV. The effect of 4-AP occurred within 1 min after application and was not reversible during the period of recording (20–30 min). On the other hand, in large neurones ($n = 4$) with TTX-sensitive, low-threshold spikes (threshold, −32 mV) 4-AP did not change the threshold (Fig. 4*B*).

4-AP also had different effects in the two populations of cells on the electrotonic potentials elicited by depolarizing current pulses. In large cells with TTX-sensitive spikes, depolarizing currents elicited potentials that exhibited a

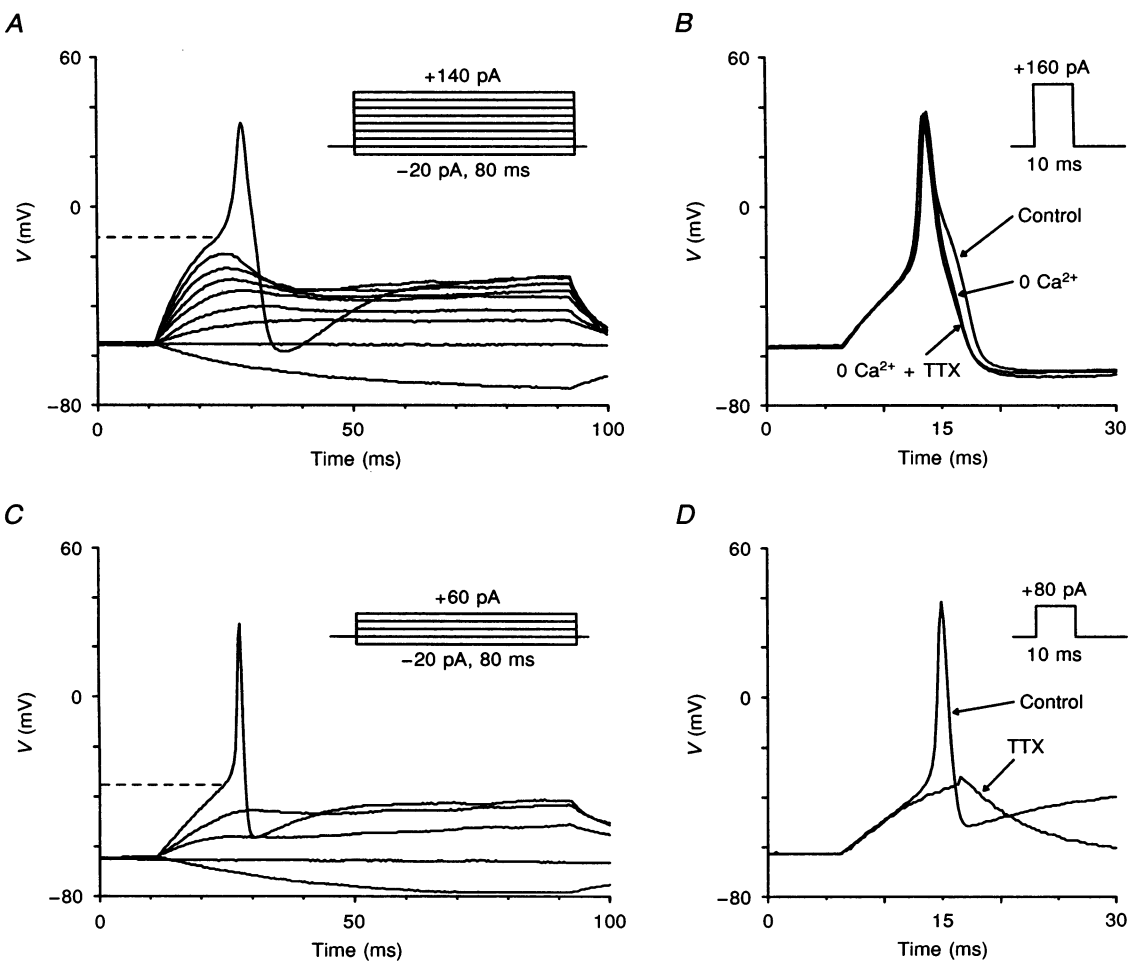

Figure 2. Action potentials in dissociated unidentified DRG neurones

Under current-clamp conditions, action potentials were evoked by depolarizing current pulses injected through the patch pipette. *A* and *B*, small-sized (21 μm) neurone; *C* and *D*, large-sized (40 μm) neurone. The small neurone exhibited a long-duration high-threshold (dashed line, −17 mV) action potential with an inflection on the repolarization phase (*A*), whereas the large neurone had short-duration lower-threshold (−37 mV) spikes with no inflection (*C*). The action potential of the small neurone, in which the spike inflection was suppressed by the removal of extracellular Ca^{2+} ions, was unaffected by the application of tetrodotoxin (TTX; 6 μM; *B*), while action potentials in the large neurone were eliminated by TTX (1 μM; *D*). Note that voltage responses in the small neurone (*A*) at membrane depolarization exceeding −45 mV exhibited a late occurring outward rectification following the peak response, whereas this did not occur in the large neurone (*C*). The pulse protocols are shown in the insets.

well-maintained plateau that was unaffected by 4-AP (Figs 2*C* and 3*C*). However, small cells with TTX-resistant spikes exhibited a marked outward membrane rectification in the depolarizing range more positive than −50 to −45 mV. The relaxation began approximately 10–15 ms after the beginning of the pulse and peaked 20–30 ms after the onset of the pulse (Figs 2*A* and 3*A*). 4-AP eliminated the outward relaxation component of the potential (Fig. 4*A*). After 4-AP treatment, the electrotonic potentials in the depolarizing range were similar in small and large cells (Fig. 4*A b* and *B b*). Figure 4*C* shows a typical example of the current–voltage (*I–V*) relationship of a FB-labelled bladder afferent neurone before and after the application of 4-AP. In this neurone, a humped action potential was elicited at a threshold membrane potential (−22 mV) and the outward relaxation of membrane potential occurred when membrane potentials were depolarized above −45 mV (Fig. 4*A*). 4-AP eliminated the membrane potential relaxation and lowered the threshold (−27 mV) for spike initiation, whereas no remarkable changes were found in the electrotonic potentials of large cells (Fig. 4*D*).

Whole-cell membrane current

Figure 5*A* and *B* shows voltage-clamp recordings of membrane currents evoked from a holding potential (−60 mV) equivalent to the physiological resting membrane potential in the neurones exhibiting TTX-resistant and TTX-sensitive action potentials, respectively. When exposed

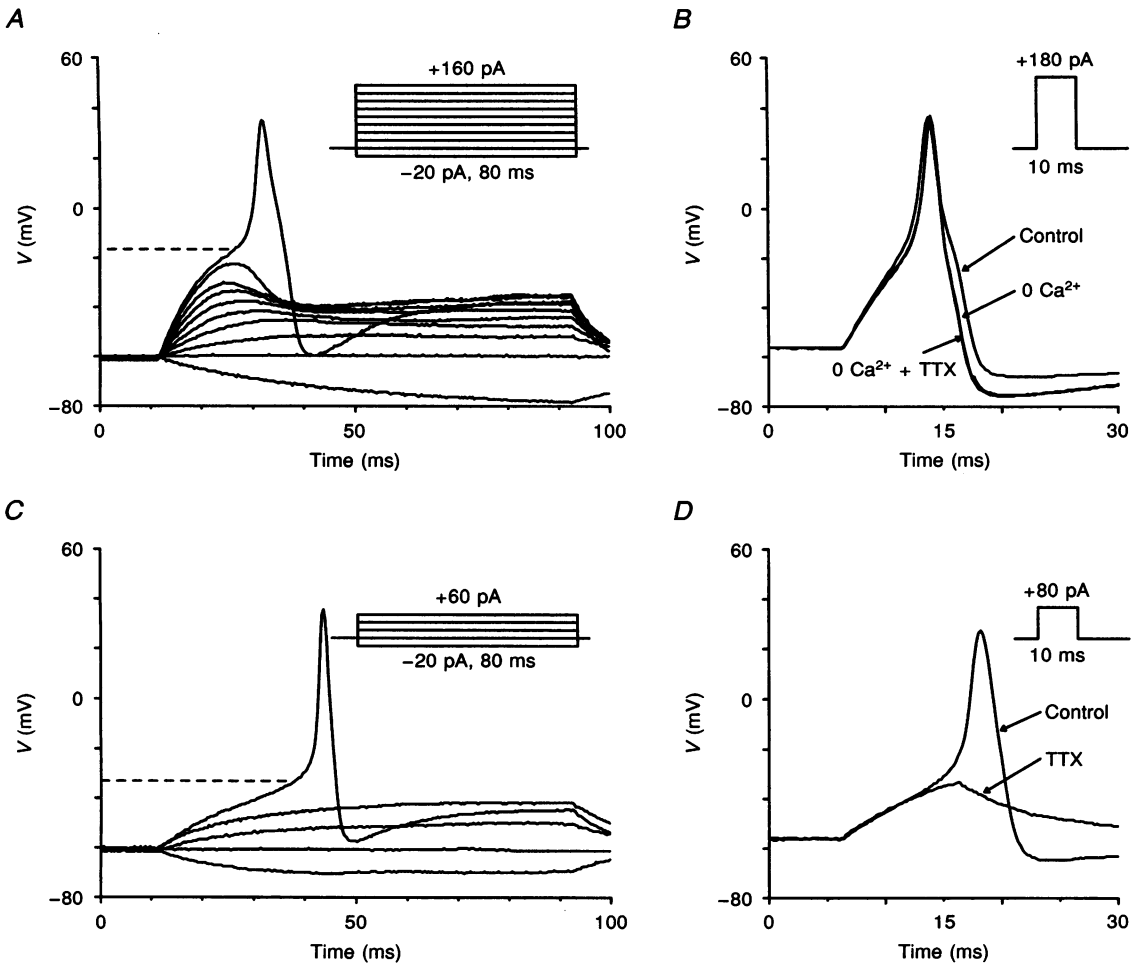

Figure 3. Action potentials in FB-labelled bladder afferent neurones

Under current-clamp conditions, action potentials were evoked by depolarizing current pulses injected through the patch pipette. *A* and *B*, small-sized (24 μm) neurone; *C* and *D*, large-sized (35 μm) neurone. The small neurone exhibited a long-duration, high-threshold (dashed line, −18 mV) action potential with an inflection on the repolarization phase (*A*), whereas the large neurone had a short-duration low-threshold (−35 mV) spike with no inflection (*C*). The action potential of the small neurone, in which the spike inflection was suppressed by the removal of extracellular Ca^{2+} ions, was unaffected by the application of TTX (6 μM; *B*), while the action potential in the large neurone was inhibited by TTX (1 μM; *D*). Note that voltage responses in the small neurone exhibited a late occurring outward rectification as described in Fig. 2. The pulse protocols are shown in the insets.

to normal external and internal solutions, fast transient inward currents and delayed outward currents were recorded in all neurones tested; however, the thresholds for activation of inward and outward currents were different between the two groups of neurones. The neurones exhibiting TTX-resistant spikes displayed high-threshold (−20 to −30 mV) inward currents and low-threshold (−40 to −50 mV) outward currents (Fig. 5*C*), while those with TTX-sensitive spikes had low-threshold (−35 to −45 mV) inward currents followed by high-threshold (−20 to −30 mV) outward currents (Fig. 5*D*). The low-threshold outward current recorded in TTX-resistant neurones was suppressed by the extracellular application of 4-AP (Fig. 6*A* and *C*). The remaining outward current after 4-AP application exhibited a threshold of activation at membrane potentials (−20 to −30 mV) similar to those necessary to activate outward currents in TTX-sensitive neurones (Fig. 6*B*). 4-AP did not alter the threshold or the magnitude of the outward currents in TTX-sensitive neurones (Fig. 6*B* and *D*). Based on these observations, it seems likely that the outward rectification of membrane potential evoked by depolarizing current pulses in TTX-resistant neurones under current-clamp conditions was due to the 4-AP-sensitive low-threshold outward currents.

Voltage-dependent Na^+ current

Since dissociated DRG neurones exhibited TTX-sensitive and TTX-resistant sodium spikes, further studies under voltage-clamp conditions were performed to analyse Na^+ currents in these neurones. The currents were isolated according to the following procedures. (1) K^+ currents were suppressed by equimolar replacement of KCl with CsCl in the internal solution and the addition of TEA in the external solution. (2) Ca^{2+} currents were also suppressed by

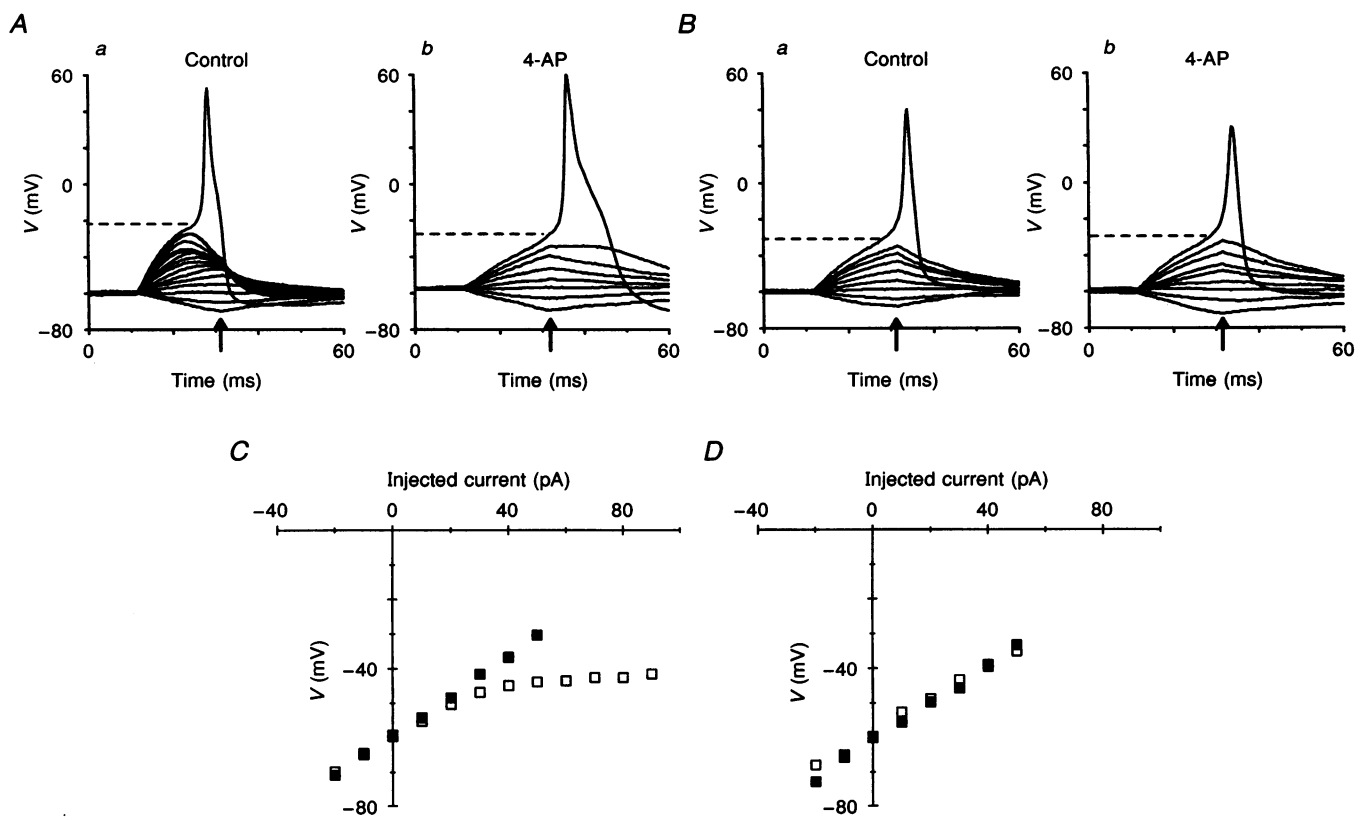

Figure 4. Effect of 4-AP on voltage responses and action potentials in FB-labelled bladder neurones

Under current-clamp conditions, voltage responses were evoked by 20 ms depolarizing current pulses injected through the patch electrode. The amplitude of the pulses was increased from −20 pA in 10 pA steps. *A*, neurone with TTX-resistant spikes; *B*, neurone with TTX-sensitive spikes. *A a* and *B a*, control; *A b* and *B b*, 4-AP (1 mM) application. Action potentials in the neurone with a TTX-resistant spike (*A*) were evoked at thresholds (dashed line) of −22 and −27 mV in the absence and presence of 4-AP, respectively, whereas no remarkable changes in spike configuration were observed in *B*. *C* and *D*, changes of membrane potentials at the end of command pulses (arrows in *A* and *B*) plotted against hyperpolarizing and depolarizing currents injected through the patch pipette, before (□) and after (■) 4-AP application in the same neurones as in *A* and *B*, respectively. Note that the relaxation of membrane potentials in the depolarizing range over −45 mV was suppressed by 4-AP application (*C*).

the reduction of external Ca^{2+} to 0·03 mM, which also reduces the influx of Na^+ ions through the Ca^{2+} channels (Elliott & Elliott, 1993). (3) The concentration of Na^+ in external solution was reduced to 100 mM by isomolar replacement with TEA to prevent the saturation of the clamp amplifier by the large Na^+ current in external solutions containing 150 mM Na^+. Under these conditions, TTX-resistant and TTX-sensitive Na^+ currents were observed in both unidentified and FB-labelled bladder afferent neurones.

Both types of current could be detected in a single neurone, and the relative proportion of TTX-resistant and TTX-sensitive components varied among cells, although certain types of neurones usually had a predominance of one type. For example, TTX-resistant Na^+ currents were primarily expressed in small-sized neurones less than 30 μm in mean diameter. Unidentified cells in which TTX-resistant current comprised more than 80% of the total Na^+ current had a mean diameter of 25·1 ± 1·4 μm ($n = 20$). In contrast, a subpopulation of unidentified cells larger than 30 μm in diameter (mean value, 32·6 ± 1·1 μm; $n = 12$) exhibited a Na^+ current that was suppressed by 70–100% following the administration of 2 μM TTX. In FB-labelled bladder afferent neurones, seventeen of twenty-one cells (mean diameter, 25·1 ± 1·3 μm) exhibited TTX-resistant currents that comprised 80–100% of the total inward current (Fig. 7*A*). The Na^+ current of the remaining four neurones (mean diameter, 32·8 ± 2·3 μm) was predominantly (> 80%) TTX sensitive (Fig. 7*B*). The mean reduction in the peak amplitude of Na^+ currents by 2 μM TTX in all twenty-one FB-labelled bladder neurones was 13·4 ± 4·1%. The TTX-resistant component of the inward currents was completely

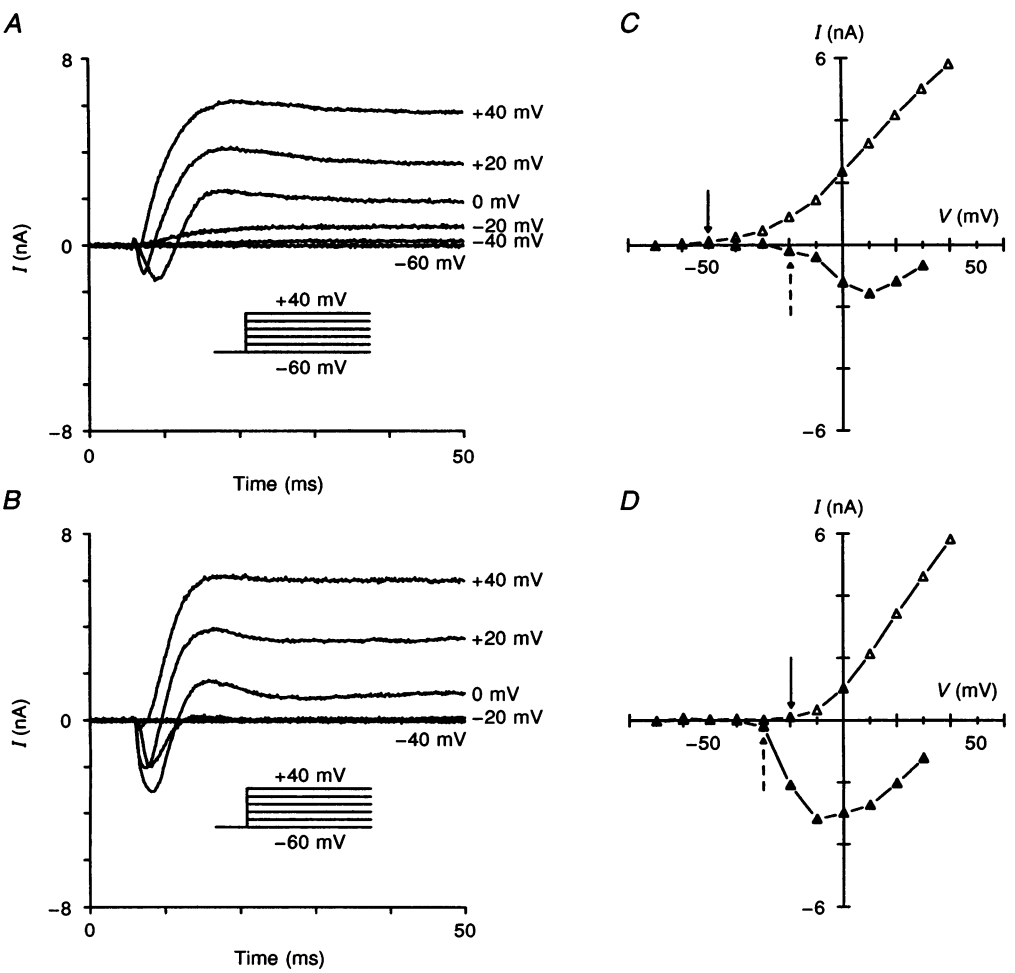

Figure 5. Membrane currents in FB-labelled bladder neurones

A, neurone with TTX-resistant spikes; *B*, neurone with TTX-sensitive spikes. Fast inward currents and delayed outward currents were elicited by depolarizing voltage steps (−60 to +40 mV) from a holding potential of −60 mV. *C* and *D*, *I–V* curves for inward and outward currents as shown in *A* and *B*, respectively. Arrows indicate thresholds for activation of either inward (dashed arrows) or outward (continuous arrows) currents. Note that outward currents were activated at a lower membrane potential (−50 mV) than inward currents (−20 mV; *C*), while inward currents (*D*) exhibited a lower threshold for activation (−30 mV) than outward currents (−20 mV).

eliminated after the removal of external NaCl, with isomolar replacement with choline chloride, indicating that Na^+ ions were the charge carrier of the TTX-resistant current (Fig. 7*A* and *B*). Bladder neurones isolated from animals pretreated with capsaicin (125 mg kg^{-1}, s.c.) had a mean diameter of 32·4 ± 2·5 μm ($n = 14$) and twelve of the fourteen cells exhibited TTX-sensitive Na^+ currents accounting for 75–100% of the total current. In all fourteen neurones obtained after capsaicin pretreatment, the reduction in the peak amplitude of the Na^+ current by the application of 2 μM TTX was considerably larger (90·3 ± 2·1%) than that in untreated animals.

Representative *I–V* curves of TTX-resistant and TTX-sensitive Na^+ currents obtained in bladder afferent neurones are shown in Fig. 7*C* and *D*, respectively. The TTX-resistant Na^+ currents were activated at potentials more depolarized than −25 mV (−25·9 ± 1·2 mV; $n = 20$) from the holding potential of −60 mV, and the reversal potential (+38 mV) was equivalent to the theoretical Na^+ reversal potential calculated by the Nernst equation. The TTX-sensitive Na^+ currents were evoked by depolarizing voltage steps from a holding potential of −70 mV. Before application of TTX, inward currents were activated with the depolarization to a membrane potential of −40 mV (−39·0 ± 1·5 mV; $n = 6$) and reached a peak amplitude at −10 mV (−13·1 ± 2·1 mV). In the presence of 2 μM TTX, a large proportion of inward currents in these cells were suppressed at all membrane potentials (Fig. 7*D*). It was also noted that the TTX-sensitive Na^+ current exhibited faster onset and decay than the TTX-resistant current. The activation and inactivation characteristics of the TTX-resistant Na^+ current were obtained from eight bladder afferent neurones in which the Na^+ current was not affected by the application of 6 μM TTX (Fig. 8). The activation curve (Fig. 8*C*) was plotted as the peak Na^+ conductance relative to the maximum conductance (g/g_{max}) *versus* the test potential (V). The data were fitted by the modified Boltzmann equation:

$$g/g_{max} = 1/(1 + \exp[(V_h - V)/k]), \quad (1)$$

where V_h is the voltage at half-maximal conductance and k is the slope factor. The values of V_h and k for TTX-resistant current activation were −10·3 and 7·8 mV per e-fold change in conductance, respectively (Fig. 8*C*). Steady-state inactivation was determined by depolarizing voltage steps to +5 mV following 1 s conditioning prepulses from −95 to −5 mV (Fig. 8*B*). The inactivation curve was plotted as the normalized peak Na^+ current amplitude (I/I_{max}) *versus* the

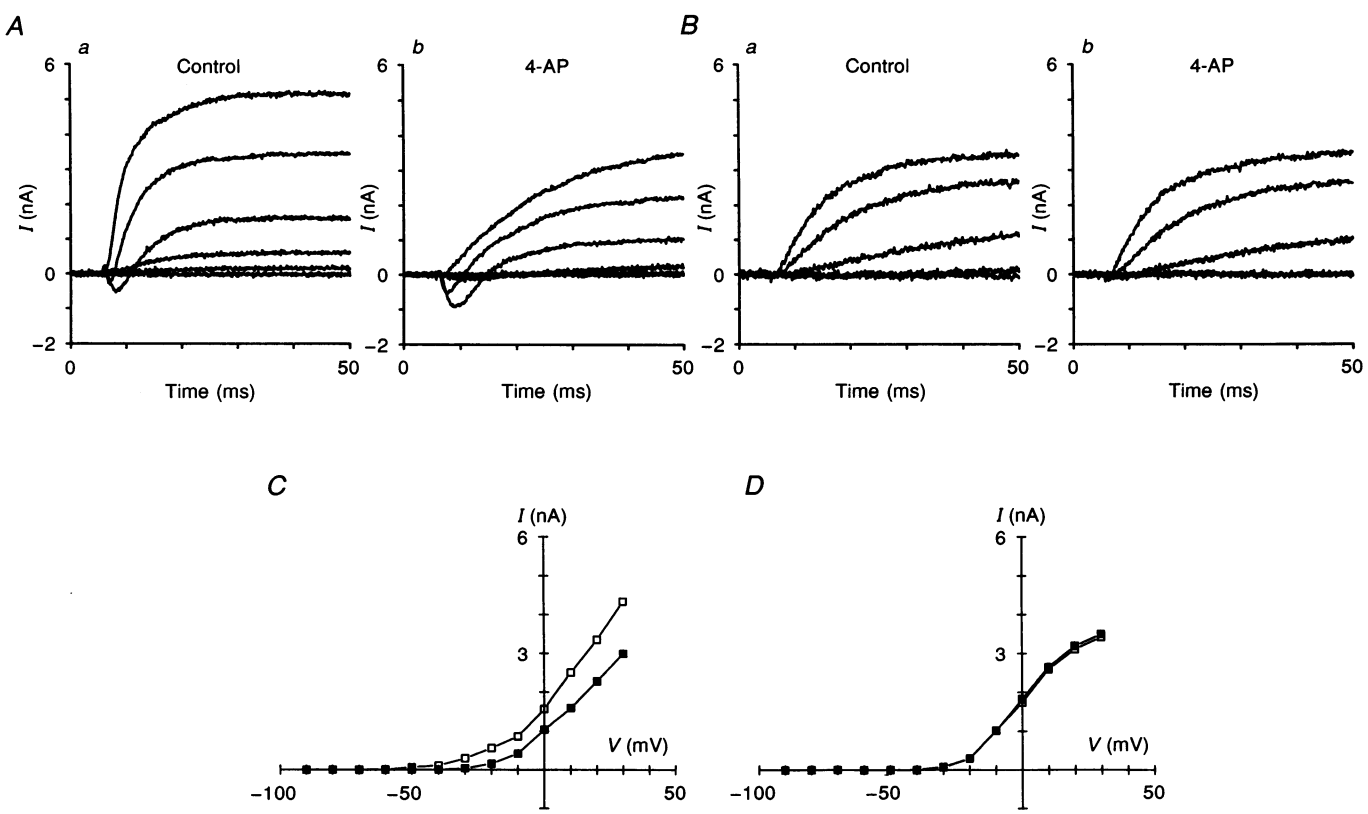

Figure 6. Effect of 4-AP on outward current in FB-labelled bladder neurones

A, neurone with TTX-resistant spikes; *B*, neurone with TTX-sensitive spikes. Outward currents elicited by voltage steps (−100 to +30 mV) from the holding potential of −60 mV were obtained in normal solution containing 1 μM TTX before (*a*) and after (*b*) 4-AP application. *C* and *D*, *I–V* curves for outward current as in *A* and *B*, respectively, before (□) and after (■) 4-AP application.

potential of the conditioning prepulses (V). The data were fitted by the modified Boltzmann equation:

$$I/I_{max} = 1/(1 + \exp[(V - V_h)/k]), \quad (2)$$

where V_h is the voltage at half-maximal amplitude of the current and k is the slope factor. The values of V_h and k for inactivation were −25·3 and 6·1 mV, respectively (Fig. 8*C*).

Activation and inactivation characteristics of the TTX-sensitive Na^+ current were obtained in eight bladder afferent neurones in which the Na^+ current was totally sensitive to TTX (Fig. 9). Activation (Fig. 9*C*) and inactivation (Fig. 9*C*) curves were plotted in the same way as described for TTX-resistant Na^+ current. According to eqn (1), the values of V_h and k for the activation curve were −25·3 and 7·0 mV, respectively. Under conditions of steady-state inactivation, the TTX-sensitive Na^+ current exhibited half-maximal inactivation (V_h) of −56 mV and a k value of 8·8 mV (Fig. 9*C*).

A-type K^+ current (I_A)

Since the low-threshold outward current of small-sized neurones exhibiting TTX-resistant spikes recorded under voltage-clamp conditions in normal solutions was blocked by the application of 4-AP, an A-channel (K_A) blocker, further experiments were performed to investigate the characteristics of this I_A current under the conditions in which Na^+ and Ca^{2+} currents were suppressed by the equimolar replacement

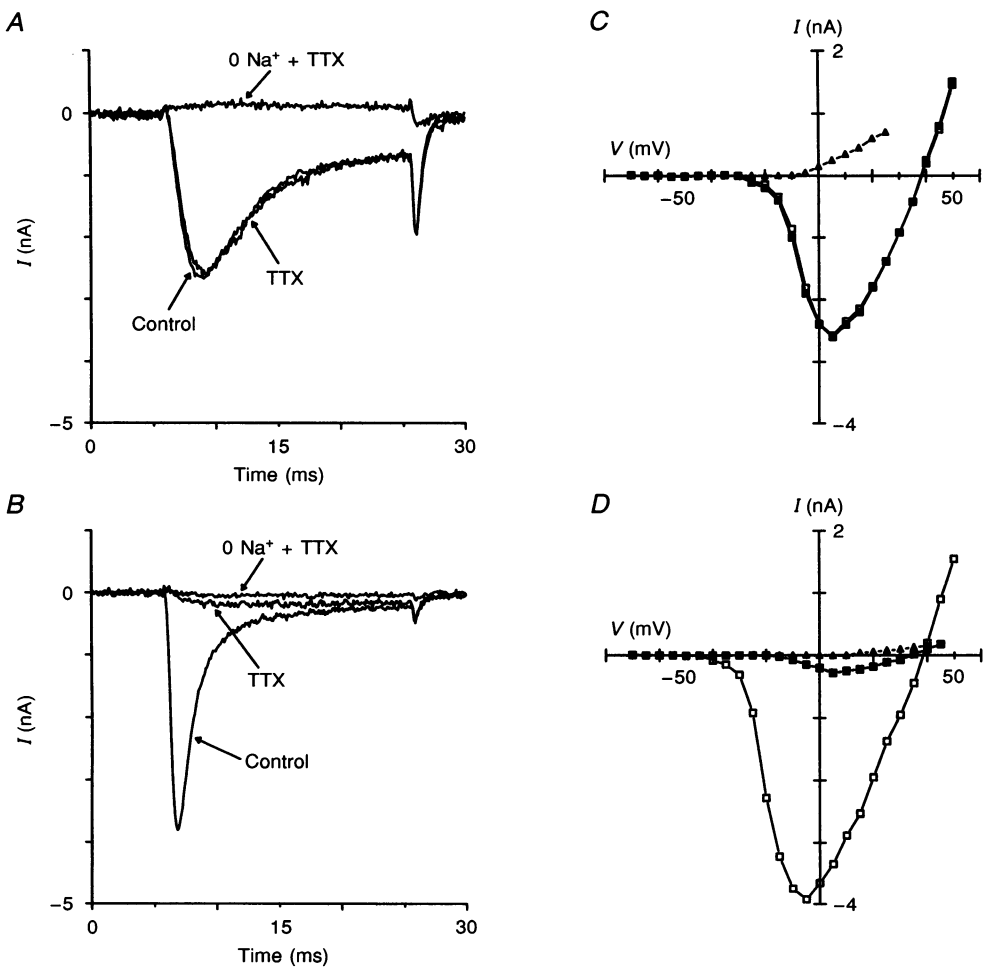

Figure 7. Na^+ currents in FB-labelled bladder afferent neurones

A, superimposed traces of Na^+ currents in a neurone with TTX-resistant spikes evoked by depolarizing voltage steps to +5 mV from a holding potential of −60 mV in the absence (Control) and presence of TTX (2 μM), and after the removal of Na^+ ions from the external solution (0 Na^+ + TTX). *B*, superimposed traces of Na^+ currents in a neurone with TTX-resistant spikes evoked by depolarizing voltage steps to −10 mV from a holding potential of −60 mV. *C* and *D*, *I–V* curves for Na^+ currents evoked by voltage steps (5 mV increments) ranging from −80 to +40 mV from a holding potential of −60 mV in the absence (□) and presence (■) of TTX, and after the removal of Na^+ ions from the external solution (△) in the same neurones as in *A* and *B*, respectively. Note that the neurones in *A* exhibited TTX-resistant Na^+ currents, while the Na^+ current in *B* was mainly TTX sensitive.

of Na^+ ions by choline and the reduction of the Ca^{2+} ion concentration to 0·03 mM in the external solution (Elliott & Elliott, 1993). The outward currents recorded under these conditions appeared to be carried by K^+ ions since the currents were totally blocked by the inclusion of Cs^+ and TEA in the internal and external solutions, respectively (Fig. 7), and the reversal potential of the instantaneous tail currents under these conditions was close (−78 mV) to the theoretical reversal potential for K^+ ions calculated by the Nernst equation.

The characteristics of fast transient I_A currents were examined in both bladder afferent neurones with TTX-resistant and TTX-sensitive action potentials. It has been reported that the I_A current, which displays voltage-dependent activation and inactivation characteristics, is largely inactivated at resting membrane potential, and can be activated when a cell is depolarized following a period of hyperpolarization (Thompson, 1977; Belluzzi, Sacchi & Wanke, 1985; Rudy, 1988). Therefore, an estimate of the I_A current was obtained by the difference in the currents activated by depolarizing voltage pulses (to +10 mV) from holding potentials of −40 and −100 mV. In this pulse protocol, the time dependence of the I_A current in neurones with TTX-resistant spikes was remarkably different from that in neurones with TTX-sensitive spikes. Figure 10*A* shows the superimposed outward K^+ currents induced by depolarization to +10 mV from different holding potentials of −40, −60 and −100 mV in a bladder afferent neurone in which the action potential was not affected by TTX. The I_A current which was obtained by the difference in the currents activated from holding potentials of −40 and −100 mV in this neurone was slowly inactivated during a 1 s depolarization and the rise (Fig. 10*B*) and decay (Fig. 10*C*) phases of the current were well fitted by single exponential curves with time constants (τ) of 2·4 ms (3·1 ± 0·2 ms; $n = 6$) and 284·3 ms (237·3 ± 9·6 ms; $n = 6$), respectively. In contrast, the I_A current in the neurones with TTX-sensitive spikes (Fig. 10*D*) exhibited faster rise time (Fig. 10*E*; mean τ, 1·2 ± 0·3 ms) and decay kinetics (Fig. 10*F*; mean τ, 20·1 ± 1·1 ms) than those in TTX-

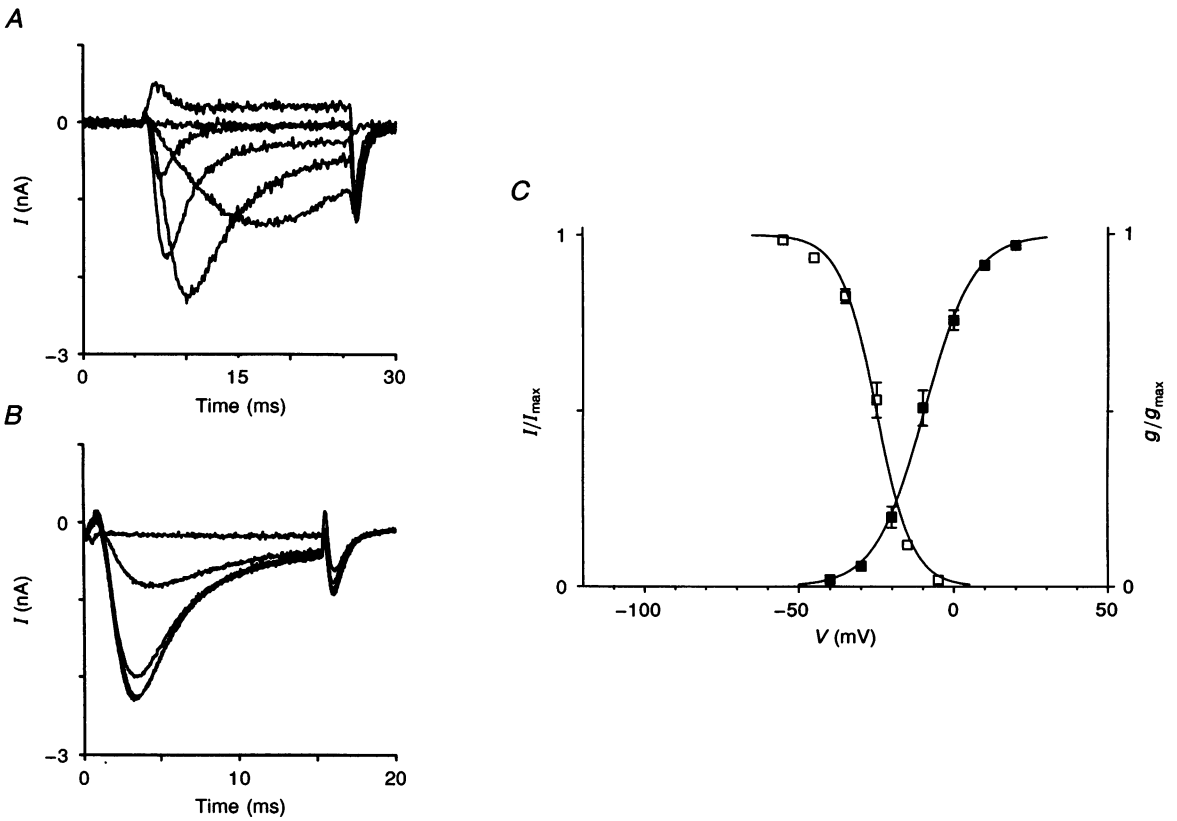

Figure 8. Voltage dependence of TTX-resistant Na^+ current in FB-labelled bladder neurones

A, Na^+ currents were elicited by depolarizing voltage steps (10 mV increments) ranging from −25 to +35 mV from the holding potential of −70 mV. *B*, steady-state inactivation of Na^+ current was examined by voltage steps to +5 mV following 1 s prepulses of −65, −45, −25, −15 and −5 mV. *C*, activation and inactivation characteristics of TTX-resistant Na^+ current obtained in 8 cells. Relative Na^+ conductances on activation normalized to the maximal Na^+ conductance (g/g_{max}; ■) and relative peak amplitude of Na^+ current on inactivation normalized to the maximal amplitude of Na^+ current (I/I_{max}; □) were plotted against membrane potential.

resistant neurones, the respective time constants being well fitted by a single exponential curve.

In addition to the difference in the time dependence, the I_A currents in TTX-resistant and TTX-sensitive neurones exhibited a different voltage dependence. In the neurones which had TTX-resistant action potentials, the I_A current could be elicited by depolarizing voltage steps (to potentials above −40 mV) from a holding potential (−60 mV) equivalent to the physiological resting membrane potential, whereas an I_A current could not be detected in TTX-sensitive neurones under the same conditions (Fig. 6). Similarly, in TTX-resistant neurones the total outward current elicited from a holding potential of −60 mV was larger than the current activated from a holding potential of −40 mV (Fig. 10*A*), at which the K_A channels are known to be inactivated (Rudy, 1988). This I_A current was not present in neurones which exhibited TTX-sensitive action potentials (Fig. 10*D*). On the other hand, both types of neurone exhibited a large increase in outward current in response to depolarizing pulses (to +10 mV) when the holding potential was shifted to −100 mV (Fig. 10*A* and *D*). The magnitude of this I_A current was determined by measuring the difference in the currents elicited at holding potentials of −40 and −100 mV. The voltage dependence of activation of the I_A current studied in this manner revealed that the I_A current in the neurones with TTX-resistant spikes was elicited by depolarizations positive to −60 mV with the half-maximal conductance (V_h) occurring at the membrane potential of −40·8 mV and with a slope factor (k) of 9·5 mV according to the modified Boltzmann equation (eqn (1); $n = 8$). V_h and k values of the I_A current activation of the neurones exhibiting TTX-sensitive spikes were −37·1 and 11·3 mV, respectively (Fig. 11*A*).

The inactivation characteristics of the I_A current were examined by a pulse protocol in which the K^+ current was activated by the depolarizing voltage step to −10 mV following 1 s conditioning prepulses ranging from −130 to −30 mV. The I_A current in the TTX-resistant neurones

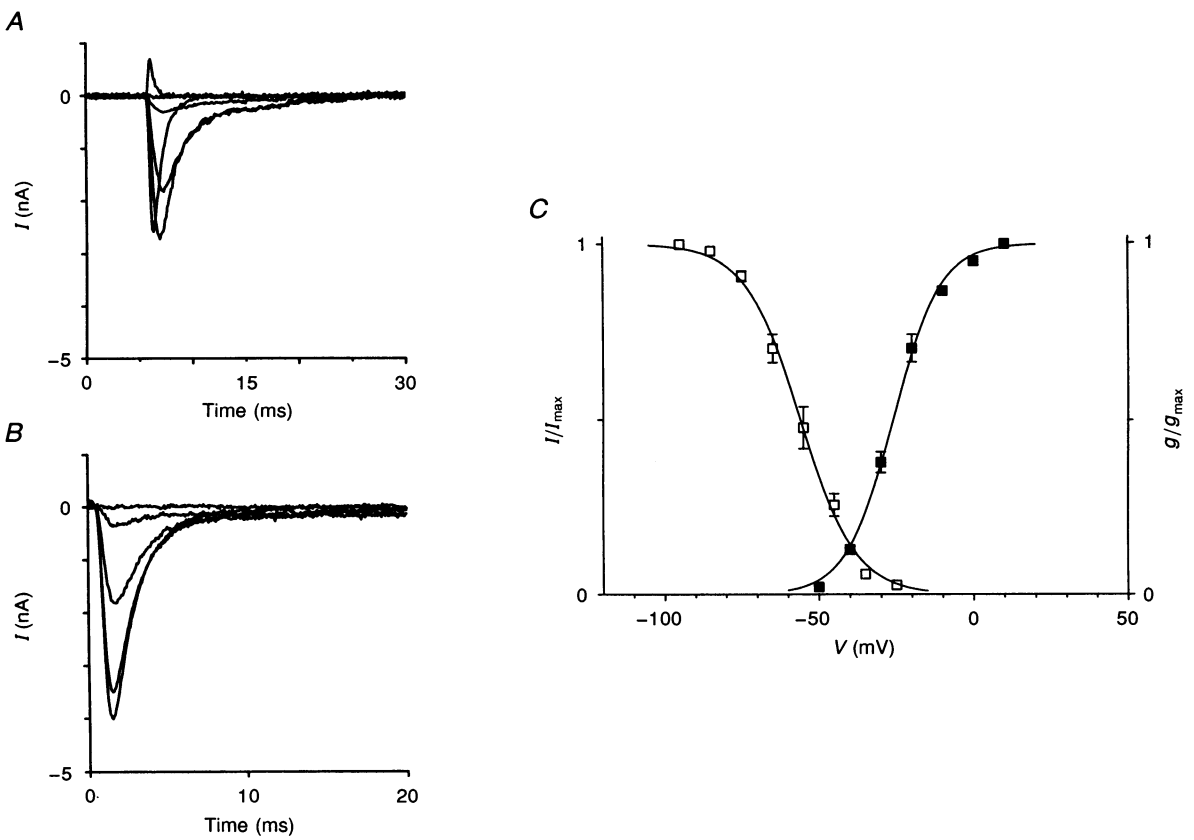

Figure 9. Voltage dependence of TTX-sensitive Na^+ current in FB-labelled bladder neurones

A, Na^+ currents were elicited by depolarizing voltage steps (10 mV increments) ranging from −45 to +35 mV from the holding potential of −70 mV. *B*, steady-state inactivation of Na^+ current was examined by voltage steps to −10 mV following 1 s prepulses of −95, −85, −65, −45, −25 and −15 mV. *C*, activation and inactivation characteristics of TTX-resistant Na^+ current obtained in 8 cells. Relative Na^+ conductances on activation normalized to the maximal Na^+ conductance (g/g_{max}; ■) and relative peak amplitude of Na^+ current on inactivation normalized to the maximal amplitude of Na^+ current (I/I_{max}; □) were plotted against membrane potential.

started to inactivate at membrane potentials positive to −110 mV and was nearly totally inactivated by depolarizing prepulses to −40 mV. The inactivation curve was plotted as the normalized peak amplitude of K^+ current (I/I_{max}) *versus* the potentials of the conditioning prepulses (V) in seven bladder afferent neurones in which action potentials were not affected by TTX. The data were well fitted by the modified Boltzmann equation (eqn (2)) with V_h and k values of −77·5 and 9·6 mV, respectively. This inactivation curve indicates that 10–20% of the maximum current could be elicited at membrane potentials in the range −60 to −50 mV, which is equivalent to the resting membrane potential level (Fig. 11*B*). In contrast, the I_A current in TTX-sensitive neurones was inactivated at more negative membrane potentials than TTX-resistant neurones. The current was almost negligible when the holding membrane potential was in the range −60 to −50 mV. Values of V_h and k for inactivation were −90·5 and 11·9 mV, respectively (Fig. 11*B*).

DISCUSSION

The present study utilized axonal tracing techniques in combination with patch-clamp recording to examine the electrical properties of L6–S1 DRG cells which innervate the urinary bladder of the adult rat. This population of visceral neurones consists of two distinct subgroups (presumably Aδ and C fibre types), which were distinguished on the basis of their morphological, electrophysiological and pharmacological characteristics. The properties of these neurones were very similar to unidentified afferent neurones of the same size in the L6–S1, as well as in thoracic and rostral lumbar (L1–L4) DRG (McLean, Bennet & Thomas, 1988; White, 1990; Caffrey, Eng, Black, Waxman & Kocsis, 1992). Since the large majority of unidentified neurones must innervate somatic target organs such as skin, striated muscle and joints, these results indicate that visceral and somatic afferents share many common features.

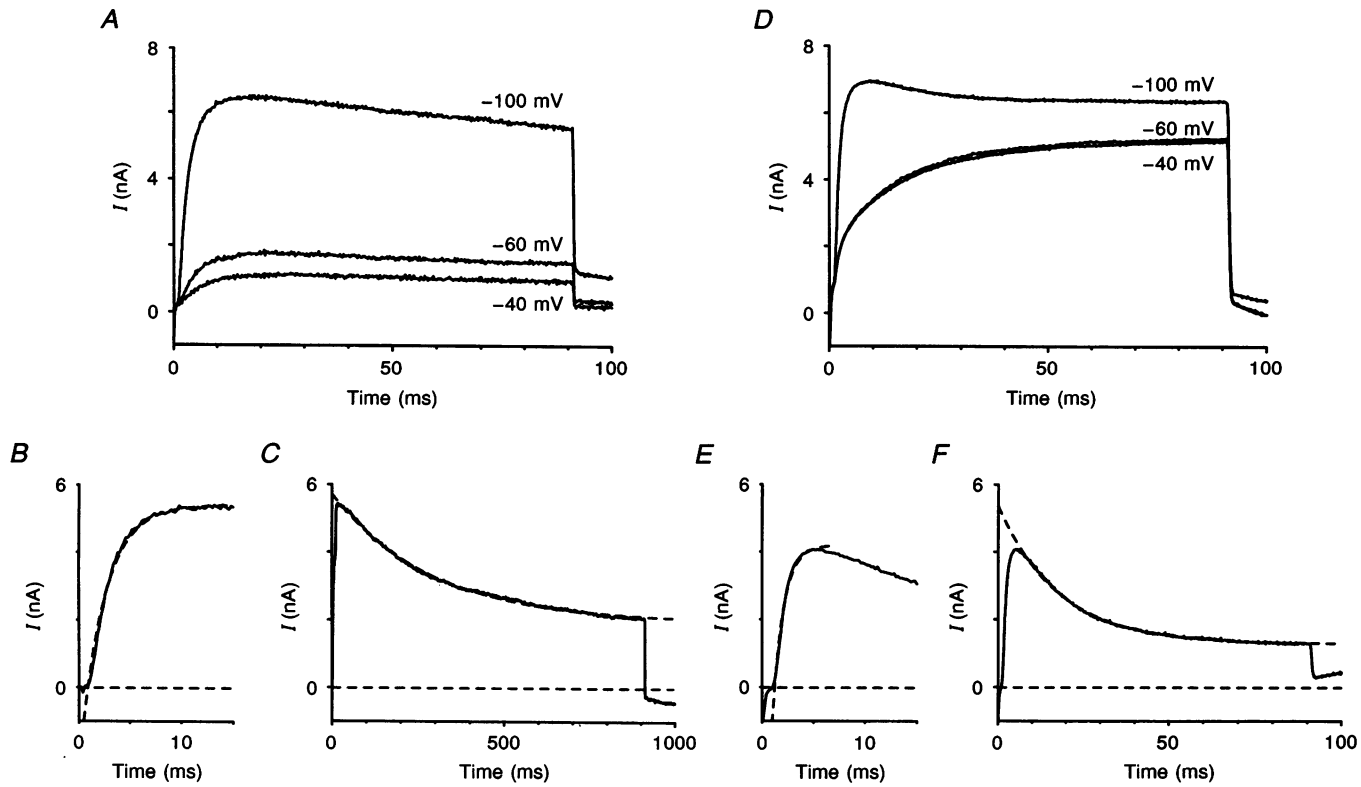

Figure 10. Characteristics of I_A current in FB-labelled bladder afferent neurones

Inward currents were suppressed by equimolar substitution of choline for Na^+ ions and reduction of the Ca^{2+} ion concentration in the external solution. *A* and *D*, outward K^+ current evoked by voltage steps to +10 mV from holding potentials of −100, −60 and −40 mV in the neurones with TTX-resistant and TTX-sensitive spikes, respectively. *B*, *C*, *E* and *F*, time dependence of rise and decay phase of I_A current in the neurones as in *A* and *D*, respectively. The current was obtained by subtraction of K^+ current evoked from the holding potential of −40 mV from that at −100 mV. The I_A current obtained from the neurone in *A* was exponentially activated with a time constant of 2·4 ms (*B*) and was not totally inactivated during the 1 s depolarizing pulse (time constant for inactivation, 284·3 ms; *C*). The I_A current in *D* was exponentially activated with a time constant of 1·05 ms (*E*) and was inactivated more rapidly (time constant for inactivation, 17·8 ms; *F*) than that of *A*.

The study of dissociated, dye-labelled bladder afferent neurones raises a number of methodological questions including: (1) are the neurones representative of the entire afferent population, and (2) does dissociation or dye labelling alter the electrical properties of the neurones? Although it is probable that a considerable proportion of the neurones are lost during enzymatic dissociation, it seems likely that the combined tracing–dissociation procedure does provide an adequate sampling of the bladder afferent neurone population. For example, the range of cell sizes and the mean cell size of the dissociated neurones are similar to the measurements of somal sizes of bladder afferent neurones in histological sections of intact ganglia (Steers *et al.* 1991; Kruse, Erdman, Puri & de Groat, 1993). In addition, the relative proportion of presumed Aδ and C fibre afferent neurones is similar to the estimated proportion of Aδ and C fibre afferent axons in bladder nerves based on electrophysiological recordings (Vera & Nadelhaft, 1990).

The question of possible changes in the properties of the neurones by dye labelling or the dissociation procedure can only be partially answered. Prolonged exposure of dye-labelled cells to UV light (Christian *et al.* 1993; Yoshimura *et al.* 1994) and exposure to high concentrations of trypsin during dissociation can elicit prominent changes in cellular properties (Lee, Akaike & Brown, 1977). However, the brief exposures (10–15 s) to UV light which were used in the present study to identify dye-labelled cells did not have a detectable effect on the electrical properties of the cells. This is consistent with the observation that dye-labelled and unlabelled cells had similar properties. Comparison of intracellular recordings in intact sensory ganglia with patch-clamp recordings of dissociated sensory neurones have also revealed similar passive and active membrane properties (Matsuda, Yoshida & Yonezawa, 1978; Ikeda *et al.* 1985; Harper & Lawson, 1985; Stansfeld & Wallis, 1985; Caffrey *et al.* 1992). Thus, it is reasonable to conclude that the data obtained from dissociated bladder afferent neurones reflects the physiological properties of these cells rather than pathological changes induced by the experimental procedures.

Bladder afferent neurones like unidentified neurones could be separated into one of two categories based on the sensitivity of the action potential and/or the Na^+ current to TTX. Although afferent neurones can exhibit both TTX-sensitive and TTX-resistant Na^+ currents, usually one type of current predominated and was responsible for the action potential. The TTX sensitivity of the action potential also correlated with other electrical and morphological characteristics of the neurone, such as somal diameter, action potential threshold

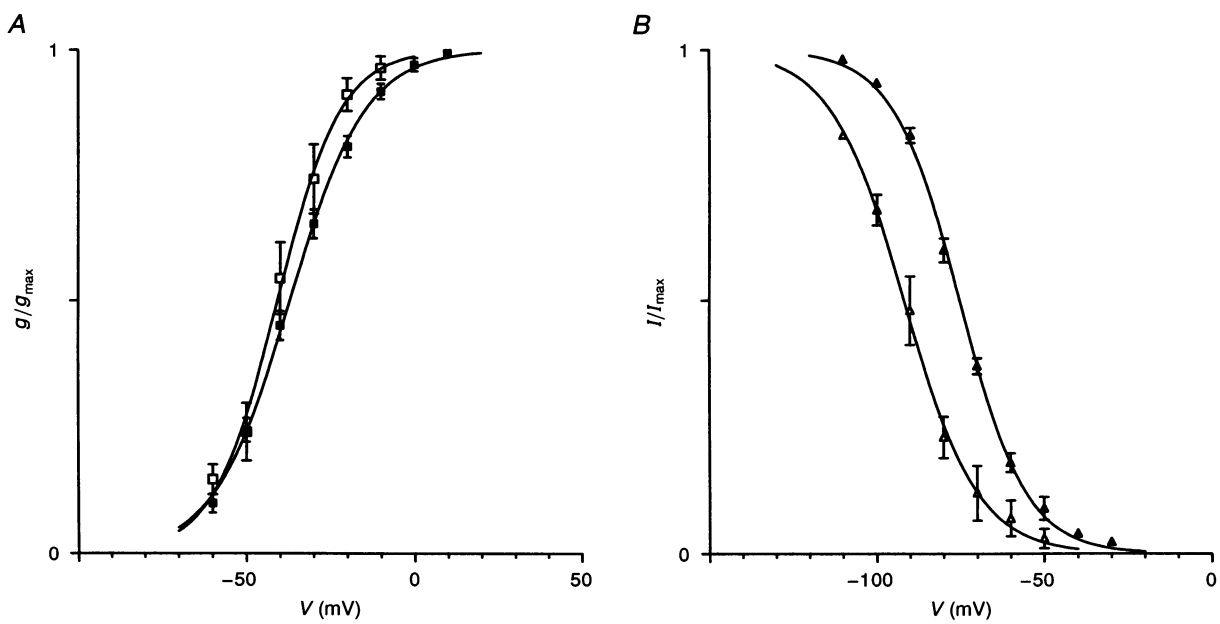

Figure 11. Steady-state activation and inactivation characteristics of I_A current in FB-labelled bladder neurones

A, activation characteristics of I_A current obtained in the neurones with TTX-resistant ($n = 8$; ■) and TTX-sensitive ($n = 7$; □) spikes. Relative I_A conductances normalized to the maximal I_A conductance (g/g_{max}) were plotted against membrane potential. *B*, inactivation characteristics of I_A current obtained in the same neurones with TTX-resistant ($n = 8$; ▲) and TTX-sensitive ($n = 7$; △) spikes. Relative peak amplitudes of I_A current normalized to the maximal amplitude of I_A current (I/I_{max}) were plotted against membrane potential. Values of V_h and the slope factor (k) were obtained by fitting curves using the modified Boltzmann equation. Note that V_h for I_A inactivation in TTX-resistant neurones (−77·5 mV) was displaced to more depolarized levels than that in TTX-sensitive neurones (−90·5 mV).

and duration, inflection on the repolarization phase of the action potential, the properties of the A-type K^+ (I_A) current, and sensitivity to capsaicin.

As noted by other investigators (Harper & Lawson, 1985; McLean *et al.* 1988; Waddell & Lawson, 1990; Caffrey *et al.* 1992), small diameter afferent neurones (< 30 μm mean diameter) tend to have TTX-resistant, long-duration, humped spikes which have a high electrical threshold, whereas larger cells have TTX-sensitive short-duration low-threshold spikes. Approximately 70% of the bladder afferent neurones are in the TTX-resistant population. The percentage of this type of cell was markedly reduced in ganglia removed from capsaicin-treated animals, suggesting that the TTX-resistant cells reflect a capsaicin-sensitive C fibre afferent population. Previous histological studies have also indicated that the capsaicin-sensitive cells represent the large majority (60%) of the bladder afferent population (Hu-Tsai, Winter & Woolf, 1992). The differential effects of the neurotoxin on the two classes of bladder neurones are not unlike the responses of unidentified afferent neurones in other sensory ganglia (Heyman & Rang, 1985; Holtzer, 1991). Thus, it seems reasonable to conclude that visceral DRG neurones innervating the urinary bladder exhibit pharmacological properties common to the general population of small-size afferent neurones.

This similarity also extends to the electrical properties of the cells. TTX-resistant bladder afferent neurones, like unidentified afferent neurones in L6–S1 DRG and in other ganglia, had broad action potentials (mean duration, 9·1 ms) with an inflection (hump) on the repolarizing phase, whereas TTX-sensitive cells had shorter-duration action potentials (5·3 ms) without the inflection. Intracellular recordings in intact DRG of adult rats showed that the broad spikes commonly occurred in the small dark cell population which includes neurones with slow-conducting unmyelinated axons (C fibre), whereas the short-duration spikes occurred in the large light cell population which includes neurones with fast-conducting myelinated axons (Aα/β). Neurones with small myelinated axons (Aδ) appear to be present in both categories. In the rat L4 DRG, all C fibre neurones and some Aβ and Aδ fibre neurones exhibited TTX-resistant spikes with an inflection of the repolarizing phase (Waddell & Lawson, 1990). If similar correlations exist in the bladder afferent population, then it would be reasonable to conclude that the majority of the cells with TTX-resistant humped spikes are C fibre neurones and that the cells with TTX-sensitive short-duration spikes are Aδ fibre neurones.

The properties of the TTX-resistant and TTX-sensitive Na^+ currents in both bladder afferent and unidentified DRG cells were markedly different. As noted in other studies (Ogata & Tatebayashi, 1992, 1993; Roy & Narahashi, 1992; Elliott & Elliott, 1993), the activation and inactivation curves for the TTX-resistant currents were displaced to depolarized levels in comparison with those of TTX-sensitive currents. For example, V_h for activation of the peak TTX-resistant current at −10 mV was 15 mV more positive than the V_h for peak TTX-sensitive current at −25 mV. However, the slope factor for activation was similar for both types of current. The V_h for inactivation was even more dramatically different being displaced to more depolarized levels by approximately 30 mV (−25 *versus* −56 mV) in comparison to the TTX-resistant current. The slope factor was also 50% greater for TTX-sensitive *versus* TTX-resistant currents. These results are qualitatively similar to those of Elliott & Elliott (1993) who studied small diameter unidentified DRG cells in the rat. However, the difference in slope factor between TTX-resistant and TTX-sensitive currents was much larger in the population of cells studied by those investigators. This difference could be due to the variation in the types of cells in the two experiments. Elliott & Elliott (1993) examined only small cells (< 25 μm mean diameter), whereas we examined a broader size range in which the cells with TTX-sensitive currents averaged 32 μm. Thus, the differences in the inactivation characteristics between TTX-resistant and TTX-sensitive currents may be exaggerated in smaller neurones.

The functional significance of the greater slope and displacement to more negative potentials of the inactivation curve for TTX-sensitive *versus* the TTX-resistant current is that the former current is likely to be inactivated over a wider range of membrane potentials and thus also exhibit a slower recovery from inactivation following an action potential. This has indeed been demonstrated by Elliott & Elliott (1993). Furthermore, a large proportion of the TTX-sensitive Na^+ channels are inactivated at the resting membrane potential in small cells. This could account for the absence of a TTX-sensitive spike in these cells. However, it has been noted in some small DRG cells that a TTX-sensitive spike can be initiated at the end of a hyperpolarizing current pulse, which presumably eliminates inactivation (Caffrey *et al.* 1992).

The properties of the I_A current in DRG neurones with TTX-resistant spikes were different from those in neurones with TTX-sensitive spikes. As described in other neurones (Thompson, 1977; Belluzzi *et al.* 1985), the I_A current in neurones with TTX-sensitive spikes was prominent when activated by membrane depolarization from a hyperpolarized holding potential and exhibited a rapid inactivation (time constant of 10 to 20 ms) following the peak of the current (for review see Rudy, 1988). Since the I_A current in neurones with TTX-sensitive spikes was almost completely inactivated at the resting membrane potential (range, −50 to −60 mV) with the half-maximal inactivation at −90·5 mV, the I_A current is unlikely to contribute to the membrane currents activated from the resting membrane potential, but should be prominent under conditions in which the cell is hyperpolarized. This is also indicated by the finding that the configuration of action potential and outward K^+ current activated from the holding potential of −60 mV in the

TTX-sensitive neurones was not altered by extracellularly applied 4-AP, a K_A channel blocker. These findings are also in line with those of Kostyuk, Veselovsky, Fedulova & Tsyndrenko (1981), that I_A currents in the DRG neurones with diameters over 30 μm were almost completely inactivated at the resting membrane potential.

In contrast, in DRG neurones with TTX-resistant spikes the application of 4-AP suppressed the outward rectification of the electrotonic potential evoked by depolarizing current pulses from holding potentials near the resting level and lowered the action potential threshold. Moreover, under the same conditions, the 4-AP-sensitive outward current in these neurones was activated at more negative membrane potentials (−50 to −40 mV) than those required to activate the TTX-resistant Na^+ current. The pulse protocol for activating these currents revealed that the I_A current in TTX-resistant neurones was more prolonged (decay time constant, 200–300 ms) than the I_A current in TTX-sensitive neurones. In addition, the V_h of the inactivation curve for I_A current in TTX-resistant neurones was displaced to more depolarized levels by approximately 15 mV than the current in TTX-sensitive neurones. Taken together, it is plausible that the slowly decaying I_A currents in small-sized DRG neurones act to suppress cell excitability by clamping the membrane potential near the resting level and thereby preventing the membrane potential from reaching the threshold for spike activation. If the C fibre afferent receptors in the urinary bladder have properties similar to those of the afferent perikarya in the DRG, this could be an explanation for the inexcitability of the silent C fibre bladder afferents.

The slowly decaying I_A current present in TTX-resistant DRG neurones is found in neonatal nodose ganglion neurones or hippocampal neurones. For example, McFarlane & Cooper (1991) reported that nodose ganglion cells have a low-threshold K^+ current, termed slow I_A, that exhibits a similar time and voltage dependence to the I_A current in TTX-resistant neurones of the present study. The slow K_A channel had a different channel conductance from that of the fast-inactivating K_A channel (Cooper & Shrier, 1989). In hippocampal neurones, the outward K^+ current, termed I_D, also had a low threshold of activation (near −60 mV) and exhibited a slow decay phase (time constant, 300–400 ms) (Storm, 1990). Both I_D and the slow I_A current were reportedly sensitive to extracellular application of 4-AP. Thus it is likely that at least two types of K_A channel differentially modulate the excitability of DRG neurones exhibiting TTX-resistant or TTX-sensitive spikes.

The different characteristics of the Na^+ channels and I_A current would therefore predict that large DRG cells would fire with a lower threshold, but would not exhibit sustained firing due to Na^+ channel inactivation, whereas small cells with TTX-resistant Na^+ channels and slowly decaying K_A channels would fire only at high thresholds, but would exhibit more sustained discharges due to less inactivation of Na^+ channels. If the properties of the cell soma reflect the properties of the peripheral afferent receptor, then these observations correlate well with the known properties of rapidly adapting, low-threshold Aδ fibre bladder afferent mechanoreceptors and tonically active, high-threshold nociceptive C fibre bladder afferents (de Groat *et al.* 1993).

In conclusion, unselected DRG neurones as well as afferent neurones innervating the urinary bladder exhibited two different types of action potential: high-threshold humped spikes in small-sized neurones and low-threshold narrow spikes in large-sized neurones. These characteristics of cell firing are regulated by the different types of Na^+ and K^+ currents. Small-sized DRG neurones were less excitable than large-sized cells due to the high-threshold TTX-resistant Na^+ channels and slow-inactivating K_A channels, which were partially active at the resting membrane potential. Large-sized DRG neurones have low-threshold TTX-sensitive Na^+ channels that are essentially unopposed by I_A currents since the fast-inactivating K_A channels are almost completely inactivated at the resting membrane potential.

Belluzzi, O., Sacchi, O. & Wanke, E. (1985). A fast transient outward current in the rat sympathetic neurone studied under voltage-clamp conditions. *Journal of Physiology* **358**, 91–108.

Caffrey, J. M., Eng, D. L., Black, J. A., Waxman, S. G. & Kocsis, J. D. (1992). Three types of sodium channels in adult rat dorsal root ganglion neurons. *Brain Research* **592**, 283–297.

Cheng, C.-L., Ma, C.-P. & de Groat, W. C. (1995). Effect of capsaicin on micturition and associated reflexes in chronic spinal rats. *Brain Research* **678**, 40–48.

Christian, E. P., Togo, J. A., Naper, K. E., Koschorke, G., Taylor, G. A. & Weinreich, D. (1993). A retrograde labeling technique for the functional study of airways-specific visceral afferent neurons. *Journal of Neuroscience Methods* **47**, 147–160.

Cooper, E. & Shrier, A. (1989). Inactivation of A currents and A channels on rat nodose neurons in culture. *Journal of General Physiology* **94**, 881–910.

de Groat, W. C., Booth, A. M. & Yoshimura, N. (1993). Neurophysiology of micturition and its modification in animal models of human disease. In *The Autonomic Nervous System*, vol. 3, *Nervous Control of Urogenital System*, ed. Maggi, C. A., pp. 227–290. Harwood Academic Publishers, London.

de Groat, W. C., Kawatani, M., Hisamitsu, T., Cheng, C.-L., Ma, C.-P., Thor, K., Steers, W. D. & Roppolo, J. R. (1990*a*). Mechanisms underlying the recovery of urinary bladder function following spinal cord injury. *Journal of the Autonomic Nervous System* **30**, S71–78.

de Groat, W. C., White, G. & Weight, F. F. (1990*b*). Patch-clamp recordings from subpopulations of autonomic and dorsal root ganglion (DRG) cells identified by axonal tracing techniques. *FASEB Journal* **4**, A1202.

Elliott, A. A. & Elliott, J. R. (1993). Characterization of TTX-sensitive and TTX-resistant sodium currents in small cells from adult rat dorsal root ganglia. *Journal of Physiology* **463**, 39–56.

Fall, M., Lindström, S. & Mazières, L. (1990). A bladder-to-bladder cooling reflex in the cat. *Journal of Physiology* **427**, 281–300.

GAMSE, R., LEEMAN, S. E., HOLTZER, P. & LEMBECK, F. (1982). Differential effects of capsaicin on the content of somatostatin, substance P, and neurotensin in the nervous system. *Naunyn–Schmiedeberg's Archives of Pharmacology* **317**, 140–148.

HABLER, H. J., JÄNIG, W. & KOLTZENBURG, M. (1990). Activation of unmyelinated afferent fibres by mechanical stimuli and inflammation of the urinary bladder in the cat. *Journal of Physiology* **425**, 545–562.

HAMILL, O. P., MARTY, A., NEHER, E., SAKMANN, B. & SIGWORTH, F. J. (1981). Improved patch-clamp techniques for high-resolution current recording from cells and cell-free membrane patches. *Pflügers Archiv* **391**, 85–100.

HARPER, A. A. & LAWSON, S. N. (1985). Electrical properties of rat dorsal root ganglion neurones with different peripheral nerve conduction velocities. *Journal of Physiology* **359**, 47–63.

HEYMAN, I. & RANG, H. P. (1985). Depolarizing responses to capsaicin in a subpopulation of rat dorsal root ganglion cells. *Neuroscience Letters* **56**, 69–75.

HOLTZER, P. (1991). Capsaicin: cellular targets, mechanisms of action, and selectivity for thin sensory neurons. *Pharmacological Reviews* **43**, 143–201.

HU-TSAI, M., WINTER, J. & WOOLF, C. J. (1992). Regional differences in the distribution of capsaicin-sensitive target-identified adult rat dorsal root ganglion neurons. *Neuroscience Letters* **143**, 251–254.

IKEDA, S. R., SCHOFIELD, G. G. & WEIGHT, F. F. (1985). Na^+ and Ca^+ currents of acutely isolated adult rat nodose ganglion cells. *Journal of Neurophysiology* **55**, 527–539.

JÄNIG, W. & KOLTZENBURG, M. (1990). On the function of spinal primary afferent fibres supplying colon and urinary bladder. *Journal of the Autonomic Nervous System* **30**, S89–96.

KEAST, J. R., BOOTH, A. M. & DE GROAT, W. C. (1989). Distribution of neurons in the major pelvic ganglion of the rat which supply the bladder, colon or penis. *Cell and Tissue Research* **256**, 105–112.

KOSTYUK, P. G., VESELOVSKY, N. S., FEDULOVA, S. A. & TSYNDRENKO, A. Y. (1981). Ionic currents in the somatic membrane of rat dorsal root ganglion neurons-III. Potassium Currents. *Neuroscience* **6**, 2439–2444.

KRUSE, M. N., ERDMAN, S. L., PURI, G. & DE GROAT, W. C. (1993). Differences in Fluorogold and wheat germ agglutinin-horseradish peroxidase labelling of bladder afferent neurons. *Brain Research* **613**, 352–356.

LEE, K. S., AKAIKE, N. & BROWN, A. M. (1977). Trypsin inhibits the action of tetrodotoxin on neurones. *Nature* **265**, 751–753.

MCFARLANE, S. & COOPER, E. (1991). Kinetics and voltage dependence of A-type currents on neonatal rat sensory neurons. *Journal of Neurophysiology* **66**, 1380–1391.

MCLEAN, M. J., BENNET, P. B. & THOMAS, R. M. (1988). Subtypes of dorsal root ganglion neurons based on different inward currents as measured by whole-cell voltage clamp. *Molecular and Cellular Biochemistry* **80**, 95–107.

MALLORY, B., STEERS, W. D. & DE GROAT, W. C. (1989). Electrophysiological study of micturition reflexes in rats. *American Journal of Physiology* **257**, R410–421.

MATSUDA, Y., YOSHIDA, S. & YONEZAWA, T. (1978). Tetrodotoxin sensitivity and Ca component of action potentials of mouse dorsal root ganglion cells cultured in vitro. *Brain Research* **154**, 69–82.

NADELHAFT, I. & BOOTH, A. M. (1984). The location and morphology of preganglionic neurons and the distribution of visceral afferents from the rat pelvic nerve: A horseradish peroxidase study. *Journal of Comparative Neurology* **226**, 238–245.

OGATA, N. & TATEBAYASHI, H. (1992). Ontogenic development of the TTX-sensitive and TTX-insensitive Na^+ channels in neurons of the rat dorsal root ganglia. *Developmental Brain Research* **65**, 93–100.

OGATA, N. & TATEBAYASHI, H. (1993). Kinetic analysis of two types of Na^+ channels in rat dorsal root ganglia. *Journal of Physiology* **466**, 9–37.

ROY, M. L. & NARAHASHI, T. (1992). Differential properties of tetrodotoxin-sensitive and tetrodotoxin-resistant sodium channels in rat dorsal root ganglion neurons. *Journal of Neuroscience* **12**, 2104–2111.

RUDY, B. (1988). Diversity and ubiquity of K channels. *Neuroscience* **25**, 729–749.

STANSFELD, C. E. & WALLIS, D. I. (1985). Properties of visceral primary afferent neurons in the nodose ganglion of the rabbit. *Journal of Neurophysiology* **54**, 245–260.

STEERS, W. D., CIAMBOTTI, J., ETZEL, B., ERDMAN, S. & DE GROAT, W. C. (1991). Alterations in afferent pathways from the urinary bladder of the rat in response to partial urethral obstruction. *Journal of Comparative Neurology* **310**, 401–410.

STORM, J. F. (1990). Potassium currents in hippocampal pyramidal cells. *Progress in Brain Research* **83**, 161–187.

THOMPSON, S. H. (1977). Three pharmacologically distinct potassium channels in molluscan neurones. *Journal of Physiology* **265**, 465–488.

VERA, P. L. & NADELHAFT, I. (1990). Conduction velocity distribution of afferent fibers innervating the rat urinary bladder. *Brain Research* **520**, 83–89.

WADDELL, P. J. & LAWSON, S. N. (1990). Electrophysiological properties of subpopulations of rat dorsal root ganglion neurons in vitro. *Neuroscience* **36**, 811–822.

WHITE, G. (1990). $GABA_A$-receptor-activated current in dorsal root ganglion neurons freshly isolated from adult rats. *Journal of Neurophysiology* **64**, 57–63.

YOSHIMURA, N. & DE GROAT, W. C. (1992). Patch clamp analysis of afferent and efferent neurons that innervate the urinary bladder of the rat. *Society for Neuroscience Abstracts* **18**, 127.

YOSHIMURA, N., WHITE, G., WEIGHT, F. F. & DE GROAT, W. C. (1994). Patch-clamp recordings from subpopulations of autonomic and afferent neurons identified by axonal tracing techniques. *Journal of the Autonomic Nervous System* **49**, 85–92.

Acknowledgements

This study was supported by an NIH Grant DK-49430.

Author's email address

N. Yoshimura: nyos+@pitt.edu

Received 5 December 1995; accepted 28 February 1996.